Pervasive translation of circular RNAs driven by short IRES-like elements

Xiaojuan Fan[1, 2] *, Yun Yang [1, *], Zefeng Wang[1, 2, #]

[1] Bio-med Big Data Center, CAS Key Laboratory of Computational Biology, CAS Center for Excellence in Molecular Cell Science, CAS-MPG Partner Institute for Computational Biology, Shanghai Institute of Nutrition and Health, [2] University of Chinese Academy of Sciences, Chinese Academy of Sciences, Shanghai 200031, China

* These authors contributed equally to this work

[#] Corresponding to: wangzefeng@picb.an.cn

Running title: Pervasive translation of circRNAs

Abstract

Circular RNAs (circRNAs) are a class of abundant RNAs with ambiguous function. Although some circRNAs can be translated through IRES driven mechanisms, the scope and functions of circRNA translation are unclear because endogenous IRESs are rare. To determine the prevalence and mechanism of circRNA translation, we developed a cell-based system to screen random sequences and identified 97 overrepresented AU-rich hexamers (>2% of all hexamers) that drive cap-independent translation of circRNAs. These IRES-like short elements are significantly enriched in circRNAs and sufficient to drive circRNA translation. We further identified multiple *trans*-acting factors that bind these IRES-like short elements to initiate translation. Using mass-spectrometry data, hundreds of circRNA-coded peptides were identified, most of which have low abundance due to rapid degradation. As judged by mass-spectrometry, 50% of endogenous circRNAs undergo rolling circle translation, several of which were experimentally validated by western blotting. Consistently, the mutation of the IRES-like short element in a circRNA reduced its translation. Collectively, our findings suggest a pervasive translation of circRNAs, providing profound implications in circRNA function.

Introduction

Circular RNAs (circRNAs) have recently been demonstrated as a class of abundant and conserved RNAs in animals and plants (for review, see [1,2]). Most circRNAs are produced from a special type of alternative splicing known as back-splicing, and are predominantly localized in cytoplasm [3-5]. However, the general function of circRNA *in vivo* is still an open question. Several circRNAs have been reported to function as molecular sponges to sequester miRNAs [6,7] or RNA binding proteins (RBPs) [8] (i.e., as competitors of the linear mRNAs), whereas some nuclear circRNAs were reported to promote transcription of nearby genes [9,10]. Since *in vitro* synthesized circRNAs can be translated in cap-independent fashion [11] and most circRNAs are localized in cytoplasm, it is highly possible that many circRNAs function as mRNAs to direct protein synthesis.

Recently we and other groups reported that some circRNAs can indeed be translated *in vivo* via different internal ribosome entry sites (IRESs) [12-15]. Because circRNAs lack a 5′ end, the translation of circRNAs can only be initiated through a cap-independent mechanism that requires the internal ribosomal entry site (IRES). However the endogenous IRESs are infrequent in eukaryotic transcriptomes, and even their existence is sometimes under debate [16-18], which casted doubts on the scope of circRNA translation. In support of this notion, a recent study has identified hundreds of putative IRESs by systematically searching selected viral sequences and

5′-UTR of human mRNA [19], however only a small fraction (<1.5%) of ~100,000 known circRNAs [20] contain these newly identified IRESs.

To study the scope of circRNA translation, we developed a cell-based reporter system to screen a random library for short sequences that drive circRNA translation. Through a near-saturated screen and subsequent bioinformatics analyses, we identified 97 IRES-like hexamers that can be clustered into 11 groups with AU rich consensus motifs. The IRES-like activities of these short motifs were further validated experimentally. Importantly, the IRES-like elements are significantly enriched in human circRNAs compared to all linear RNAs, suggesting that they are positively selected in circRNAs. Since these IRES-like hexamers account for ~2% of all hexamers (97/4096), any sequences longer than 50-nt should contain such an element by chance, implying that most circRNAs in human cells can potentially be translated through the IRES-like short elements. Consistently, we found that circRNAs containing only the coding sequences can indeed be translated in a rolling circle fashion, presumably from internal IRES-like short elements in the coding region. We further identified hundreds of circRNA-coded proteins with mass spectrometry datasets, and explored the potential roles of the circRNA-coded proteins and the mechanism of their translation. Collectively, our data indicate that short IRES-like elements can drive extensive circRNA translation, which may represent a general function of circRNAs.

Result

Unbiased identification of short IRES-like elements

Previously we reported that GFP-coding circRNAs can be translated from different viral or endogenous IRESs [12,13]. Surprisingly, three of the four short poly-N sequences used as negative controls for known IRESs were also found to promote GFP translation, with the only exception of poly-G (Fig. S1A). This observation indicates that certain short elements other than known IRESs are sufficient to initiate circRNA translation. To systematically identify additional sequences that drive circRNA translation, we adopted an unbiased screen approach originally developed to identify splicing regulatory *cis*-elements [21-23]. Briefly, a library of random 10-nt sequences was inserted before the start codon of circRNA-coded GFP [24], which was transfected into 293T cells to generate circRNAs that can be translated into intact GFP (see Methods and Table S1). The cells with active circRNA translation (i.e. green cells) can be recovered with fluorescence activated cell sorting (FACS), and the inserted decamers can be subsequently sequenced to identify the IRES-like elements that drive circRNA translation.

To achieve full coverage of entire library, >100 million cells were transfected (Fig. 1A). We sequenced the inserted fragments from both dark and green cells using high-throughput sequencing, and compared the resulting decamers between these two cell populations to extract the hexamers enriched in the green cells *vs.* the dark cells (Fig. 1B). We have identified 97 hexamers that are significantly enriched in the cells with GFP fluorescence (Table S2). These enriched sequences are generally AU-rich

despite the pre-sorting library has roughly even base composition (Fig. 1C and Fig. S1B). In addition, these hexamers have strong dinucleotide biases toward AC, AG, AT and GA (Fig. 1D). Based on sequence similarity, the 97 hexamers enriched in green cells were further clustered into 11 groups to produce consensus motifs (Fig. 1E, top). Most consensus motifs are AU-rich motifs and enriched in 3′-UTR of linear mRNA (Fig. S1C). Consistent with the previous report that m6A modification sites can function as IRES to drive circRNA translation [13], several enriched hexamers contain the RRACH signature for the m6A modification, however they were not prevalent enough to be clustered into a consensus motif.

The IRES-like activities of each cluster were further validated by inserting the representative hexamers (or the control hexamers depleted in green cells) into the circRNA reporter to examine the translation product of the resulting circRNAs (Fig. 1E, bottom). All the reporters inserted with the enriched hexamers showed robust GFP translation from circRNAs, whereas the GFP productions from the reporters inserted with control hexamers were barely detectable (Fig. 1F). The circRNA levels were similar in all reporters containing different hexamers as judged by RT-PCR and by northern blot (Fig. 1E, 1F and Fig. S1D-E), suggesting that the differences in GFP production are probably due to distinct activities of these hexamers in driving translation rather than by differences in back-splicing efficiency. Collectively, these results indicated that our screen can reliably identify short sequences that drive circRNA translation, and thus we refer this set of 97 hexamers as IRES-like hexamers.

IRES-like hexamers are enriched in endogenous circRNAs to drive translation

We further examined the frequency of each hexamer in linear mRNAs and circRNAs, and compared the average frequency of the IRES-like hexamers *vs.* the control set of hexamers in different types of RNAs. In the linear mRNAs (all annotated mRNAs from RefSeq), the average frequencies of the IRES-like hexamers were similar to the random hexamers or the hexamers depleted in green cells (Fig. 2A, left panel). Surprisingly, the average frequencies of IRES-like hexamers were significantly higher in all tested circRNA datasets [3,7,25,26] compared to the control hexamer sets (Fig. 2A), indicating that endogenous circRNAs are enriched with short IRES-like elements. Since these IRES-like hexamers were independently identified from unbiased screen of random sequences, such enrichment strongly suggests that circRNAs may be positively selected for their ability to be translated.

The 97 IRES-like hexamers account for ~2% of the entire hexamer population (4^6=4096), indicating that there will be an IRES-like hexamer in a 50-nt sequence by chance. Since >99% circRNAs are longer than 100-nt [20] (Fig. S2A), most circRNAs should contain internal IRES-like short elements by chance. Therefore, almost all open reading frames (ORFs) in circRNAs could potentially be translated using such IRES-like short elements. To directly test this surprising conclusion, we generated a series of GFP-coding circRNA reporters without known IRES sequences or stop codon to measure GFP production using western blot (Fig. 2B). Consistent with our previous report, the control reporter containing the m6A modification sites at

upstream of the start codon was reliably translated [13], and deletion of stop codon in this reporter led to production of GFP concatemers through the rolling circle translation of circRNA (Fig. 2B). When deleting all untranslated sequences between the start and stop codon in the circRNA, the intact GFP translation is abolished, presumably because there is no room for any sequences to function as the IRES. However, when deleting the stop codon, the circRNA containing only the GFP coding sequence can also be translated in a rolling circle fashion to produce GFP concatemers, presumably through an internal sequence function as an IRES (lanes 4 and 5, Fig. 2B). As a control, we also confirmed the efficient circRNA expression in all the RNA samples using northern blot with the optional RNase R treatment (Fig. S2B). Interestingly, the rolling circle translation can produce some huge GFP concatemers that are retained in loading wells (lanes 3 and 5, Fig. 2B, the huge proteins could not be efficiently transferred to the membrane and thus being underestimated). To eliminate the possible artifacts from rolling circle transcription of circular plasmid, these reporter plasmids were stably inserted into genome using Flp-In system, and the similar rolling circle translations were observed in these stably transfected cells (Fig. S2C).

In addition, the rolling circle translation initiated from internal coding sequence is not limited to the GFP gene, as the circRNAs containing only the ORF sequences of different luciferase genes can also be translated from internal coding sequence (Fig. 2C, Fig. S2D-F). Interestingly, the rolling circle translation from circRNAs apparently produced more proteins than the circRNAs with stop codons (Fig. 2B),

suggesting that initiation of circRNA translation may be the rate-limiting step as the ribosome recycling and reinitiation is unnecessary for rolling circle translation [27,28].

Trans-acting factors that bind to IRES-like short elements to promote circRNA translation

With the identification of multiple IRES-like short elements, we next seek to determine the molecular mechanisms by which these elements initiate cap-independent translation of circRNA. An earlier report showed that short sequences may function as IRES by pairing with certain regions of 18S rRNA (i.e. active region) [19]. However, we found little correlation between our newly identified IRES-like elements to these "active 18S rRNA regions" (Fig. S3A), suggesting that these newly identified elements may not function by paring with 18S rRNA.

Previously we found that m6A reader protein YTHDF3 can recognize N6-methyladenosine in circRNA to directly recruit translation initiation factors [13]. By analogy we hypothesized that the newly identified IRES-like short elements may also function as regulatory *cis*-elements to recruit *trans*-acting factors that promote translation [29]. To identify such *trans*-acting factors, we used the consensus sequences of IRES-like elements as bait for affinity purification of their specific binding proteins (Fig. 3A). Briefly, the chemically synthesized 20-nt single-strand RNA oligonucleotides containing three copies of IRES-like hexamers and a 5′ end biotin modification were incubated with HeLa cell extracts, and the RNA-protein complexes were purified with streptavidin beads [21-23] (Fig. 3A). We found that, all the five

RNA probes consist of IRES-like elements showed robust binding of several proteins, whereas the negative sequence (ACCGCG) had weak background of non-specific RBP binding (Fig. 3B). The specific protein bands in each lane were collected and subsequently analyzed with mass-spectrometry (LC-MS/MS), and the top candidates in each band were identified as candidate *trans*-acting factors (Fig. 3B).

In total 58 protein candidates were identified with high confidence, with many overlapping proteins in different baits (Table S3). The majority of these proteins are known to bind RNAs and can be clustered into two major groups based on the protein-protein interaction (PPI) network: the proteins involved in RNA processing (e.g., hnRNPs) and the proteins involved in mRNA translation (e.g., the ribosomal proteins) (Fig. 3C). The identified RBPs are enriched for regulatory function in RNA processing, splicing, transport and stabilization as judged by gene ontology analysis (Fig. S3B).

To validate the function of these proteins, we fused the candidate RBPs to a programmable RNA binding domain (i.e., Puf domain) that can be designed to bind any 8-nt RNA sequences [30], and co-expressed the fusion proteins with the circRNAs containing their cognate targets. We found that the specific tethering of PABPC1 and hnRNP U clearly promoted translation of the circRNA, whereas the ELAVL1 (HuR) and hnRNP A1 did not affect translation when tethered to the same site (Fig. 3D). Such translation promoting activity required the specific binding of *trans*-acting factors to circRNAs, as disrupting the Puf-RNA interactions had abolished the

regulatory effect and restoring the specific interaction can rescue the translation-promoting activity (Fig. 3D).

PABPC1 is an abundant protein that binds to poly-A or AU-rich sequences [31]. We further examined the role of PABPC1 in regulating circRNA using reporters contain short poly-A elements at upstream of start codon in circRNA (Fig. 3E). The results showed that over-expression of PABPC1 can indeed promote translation of circRNA-coded GFP. As controls, the circRNA translation was not affected by another poly-A binding protein PABPC4 or by PTBP1 that was previously reported to enhance IRES activity (Fig. 3E). Interestingly, for unknown reason, the co-expression of U2AF2 seemed to inhibit translation of the circRNA (Fig. 3E). Taking together, our results showed that certain RBPs (e.g., PABPC1) are capable to recognize these IRES-like elements to promote cap-independent translation of circRNAs, exemplifying a new model for circRNA translation initiation independent of canonical IRESs.

Identification of circRNA-coded proteins

Since most circRNAs can potentially be translated, we further examined molecular characteristic of the putative circRNA-coded proteins. In accordance with previous observation [15], we found that the exons in the 5′ end of a pre-mRNA are more likely to be included in the circRNAs (Fig. 4A), suggesting that many circRNAs could potentially code for N-terminal truncated protein isoforms of their host genes. Consistently we found that 79% of circRNA exons are from coding region, while 17%

of circRNA exons spanning 5′-UTR and coding region and 4% spanning coding and 3′-UTR region (Fig. 4A inset).

Using the dataset of full length human circRNAs [26], we examined the putative circRNA-coded ORFs that are longer than 20 amino acids (equivalent to 60-nt). We found that a large fraction of endogenous circRNAs (67%) can code for proteins overlapping with their host genes (i.e., translated in the same reading frame as the host gene), including 14% of endogenous circRNAs that can be translated in a rolling circle fashion (named as overlapped cORF and rcORF respectively, purple pie slices in the left panel of Fig. 4B). In addition, 16% of human circRNAs can code for proteins that are different from host genes but are homologous to other known proteins (homologous cORF and rcORF, brown pie slices in Fig. 4B, left panel), whereas 10% circRNAs code for proteins that are not homologous to any known proteins on earth. In fact, only 7% of circRNAs have no ORF longer than 20 aa. In comparison, a much larger fraction of circRNAs from two different controls (reversed or shuffled sequence controls) do not contain ORFs longer than 20 aa (Fig. 4B, right two panels), and the remaining control circRNAs are more likely to code for proteins that are not homologous to any known proteins, suggesting that the endogenous circRNAs are more likely to code for functional proteins compared to controls.

To systematically identify circRNA-coded proteins, we searched raw mass spectra from publically available tandem mass spectrometry (MS-MS) datasets for possible peptides across the back splice junctions of all published circRNAs [20,26] (Fig. 4C). Two sets of high-resolution comprehensive human proteomic data were selected,

including raw mass spectra data from 30 tissues and 6 cell lines [32,33]. We used open pFind(v3.1.3) [34] to search against a combined database of UniPort human proteins and potential peptides encoded by back splice junctions of circRNAs. We applied fairly stringent thresholds (see Methods) to identify the peptides that are encoded only by back splice junctions of circRNAs but not found in any known proteins. Two additional filters were used to reduce false positives in our search: We discarded peptides similar to canonical proteins in non-redundant human protein database (0-2 mismatches), and required the positive spectra to contain peptide fragments encoded by both sides of back splice junction.

Our search of endogenous circRNA-coded proteins identified 2721 mass spectra across 990 back splice junctions from 646 human genes, all of which contain putative cORF or rcORF longer than 20 amino acids (Fig. 4D, Table S4). Interestingly, we found that the fraction of circRNAs with rolling circle translation products increased as the additional filters were applied in our search (~50% of the circRNAs contain putative rcORFs at the end, see Fig. 4D). More than 80% of the identified circRNA-coded peptides overlapped with the translation products of their host genes (Fig. 4D), suggesting that the circRNAs preferably produce different translation isoforms of the host genes. Interestingly, the gene ontology analyses of their host genes indicated that these genes are significantly enriched with the functions in RNA translation, RNA splicing/processing, and platelet degranulation (Fig. S4). Such functional enrichment implies that many circRNAs may code for new protein isoforms that play potential roles in regulating these biological processes. In

addition, the enrichment in platelet degranulation may also provide a functional implication to the previous observation that the circRNAs are highly expressed in platelet [35,36].

For many circRNAs, we identified multiple mass spectra to support the same back splice junctions, including 80 circRNAs with >10 different spectra across their back splice junctions (Fig. 4E). Further analyses showed that the circRNA-coded peptides are mostly presented in a small set of cells or tissues, with 60-80% of circRNA-coded peptides being identified only from a single sample in both MS-MS datasets (Fig. 4F, blue bars). In comparison, the peptides encoded by the adjacent splicing junctions from the linear mRNAs are more ubiquitously expressed, with some peptides being found in all samples (Fig. 4F, grey bars). These results suggest that the circRNA-coded proteins are generally more specific to certain cell types or tissues.

circRNA-coded proteins have relatively low abundance due to rapid degradation

We next analyzed the numbers of mass spectra supporting circRNA-coded peptides (i.e. peptides across back splice junctions) in all samples and compared to those from known proteins encoded by the canonical linear mRNAs. As expected, the numbers of newly identified circRNA-coded peptides were positively correlated with the numbers of total peptides in two independent datasets (Fig. 4G). In addition, applying additional fractionations in the same sample (e.g., 39, 46 and 70 fractions of HeLa cells) increased the numbers of newly identified circRNA-coded peptides (Fig.

4G). These results suggested that the proteomic identifications of circRNA-coded proteins have not reached saturation, and thus the spectrum numbers of supporting peptides will be roughly correlated to the abundance of these "new proteins".

To estimate the relative abundance of circRNA-coded proteins, we compared the peptides across back splice junction *vs.* those across adjacent splicing junctions of the host linear mRNA. We found that the circRNA-coded peptides generally have a smaller number of spectra to support each peptide as compared to those from the peptides encoded by linear adjacent splice junctions (Fig. S5A), suggesting that the circRNA-coded peptides have much lower abundance than their linear counterparts. Consistently, the q values of the mass spectra supporting circRNA-coded peptides were much higher than those supporting the peptides across linear adjacent splice junctions (Fig. S5A). Since the more abundant proteins are usually supported by MS data with higher confidence, this result again suggested that the circRNA-coded proteins generally have lower abundance than their linear counterparts.

In addition, even for the canonical proteins, we can only detect a small number of peptides across the splice junctions using MS-MS data (4254 out of 67912 adjacent canonical junctions) (Fig. S5A). By analyzing the sequence composition across splicing junctions, we found that lysine and arginine are enriched at the -1 position of all splicing junctions (Fig. S5B). Specifically, >70% of splice junctions contain at least one lysine or arginine regardless of linear or back splice junctions (data not show). Since the current proteomic samples are mostly lysed by trypsin with a cleavage site of lysine or arginine, such sequence bias leads to a significant depletion

of peptides across splice junctions. Unlike the proteins encoded by linear mRNAs, the circRNA-coded proteins can only be recognized by peptides across back splice junctions, which could partially explain why the circRNA-coded peptides are difficult to identify. This result further suggested that additional circRNA-coded proteins could be identified by optimizing MS methods with different protease cleavage.

The low abundance of circRNA-coded proteins is probably due to a slow protein synthesis from cap-independent translation and/or a fast protein degradation. It is previously known that the efficiency of cap-independent translation is relatively low, which partially explained the low abundance of circRNA-coded proteins. However, the stability of the circRNA-coded proteins is still an open question: Although the majority of circRNA-coded protein sequences overlap with the proteins encoded by endogenous host gene, it is possible that the extra peptides specifically encoded by sequences across the back-splicing junction make the protein unstable.

To directly address this possibility, we selected three C-terminal peptides specifically encoded by the sequences across the back splice sites of different circRNAs, and fused them to the C-terminus of GFP in the circGFP reporters (Fig. S5C). The resulting circRNA will code for a GFP fusion protein containing different circRNA-specific peptides, and we found that these GFPs with circRNA-coded tails are expressed in much lower level compared to the one without these tails (Fig. S5D). Moreover, the expression level of the fusion proteins with circRNA-coded tails increased upon the inhibition of proteasome degradation by MG132 treatment, whereas the GFP without such tails was essentially unaffected (Fig. S5E). In

contrast, the levels of all GFP fusion proteins were not affected by chloroquine treatment that inhibits autophagic protein degradation (Fig. S5E). These observations indicate that the circRNA-coded C-terminal tails can indeed destabilize many circRNA-coded proteins, and such degradation was mainly mediated by proteasomes.

Translation products derived from circRNAs

Although the endogenous circRNAs were found to contain more cORFs (with the cORF:rcORF ratio roughly equaling to 3.4, Fig. 4B), further analyses of proteomic data showed that about half of the circRNA-coded peptides are derived from the endogenous circRNAs containing rcORFs (Fig. 4D), suggesting that rcORFs are more efficiently translated from circRNAs (consistent with observations in Fig. 2B and 2C). Since the endogenous circRNAs had not been reported to undergo rolling circle translation, we seek to further determine whether these identified circRNAs with rcORFs are indeed translated in different cells.

We selected three circRNAs (circPSAP, circPFAS, and circABHD12) with high quality mass spectra across back splice junctions (Fig. 5A), and constructed back-splicing reporters to ectopically express these circRNAs in two different cell types [24]. A V5 epitope tag was also inserted into the same reading frame of rcORFs to facilitate the detection of the translation products by western blot (Fig. 5B). We found multiple protein bands in 293T and SH-SY5Y cells transfected with all circRNAs tested, suggesting that these circRNAs undergo robust rolling circle translation to produce protein concatemers (Fig. 5C and Fig. S6A). Interestingly, the

cells transfected with circPSAP reporter produced a faint band of protein concatemer and a much stronger band corresponding to the product of a single cycle of circRNA translation, suggesting a low translation processivity for this circRNA.

Since the translation of rcORFs can generate protein concatemers with repeat sequences, they are likely to induce mis-folding and aggregation of proteins, which often leads to rapid protein degradation. To measure the stability of theses proteins translated from rcORF, we transfected cells with these circRNA reporters and treated the cells with short exposure of MG132 or chloroquine. We found that the translation products of two circRNAs (circPSAP and circPFAS) were increased by MG132 treatment but not by chloroquine in two different cells (Fig. 5D), whereas the ectopically expressed control protein GFP was not affected, suggesting that the rolling circle translation products were rapidly degraded in cells through proteasome pathway. These findings are consistent with the observation that the circRNA-coded proteins are generally low abundant inside cells (Fig. S5). Intriguingly, the translation product of circABHD12 seems to be relatively stable despite containing repetitive sequences (i.e., not affected by brief treatment with MG132 or chloroquine).

Next, we seek to examine whether the rolling circle translation of endogenous circRNAs is indeed driven by the newly identified IRES-like short elements. We selected the circPFAS that contains two IRES-like hexamers, and made individual mutations on both hexamers to examine if such mutations can affect its translation (Fig. 5E, the other two circRNAs contain 3, and 10 IRES-like hexamers and thus were not tested). We found that the mutation on one of the IRES-like hexamers

(AAGAAG) dramatically reduced the translation of circPFAS, whereas the mutation on the other element (AATTCA) had no effect on translation, suggesting that the AAGAAG hexamer is the major translation initiation element in circPFAS (Fig. 5E and Fig. S6B). Interestingly, residue amount of translation product was observed even with mutations on both IRES-like elements, suggesting that other unknown *cis*-elements may also help to promote circPFAS translation. This observation is not a surprise since we used a strong cutoff (enrichment z score >7) in the identification of the 97 IRES-like hexamers, and thus may miss some elements with weak IRES-like activity.

We next examined if the rolling circle translation of endogenous circPFAS can also be affected by the *trans*-acting factors that promote cap-independent translation of circRNA reporters (Fig. 3D and 3E). To this end, we co-expressed the circPFAS with PABPC1, hnRNP A1, hnRNP U, or ELAVL1 in two different cell types (293T and SH-SY5Y cells), and measured the products of rolling circle translation with western blot. We found that all tested *trans*-acting factors significantly increased the rolling circle translation products from circPFAS (Fig. 5F and Fig. S6C). This observation suggest that the same set of *trans*-acting factors identified earlier (Fig. 3) may also promote the rolling circle translation of endogenous circRNA, and that the translation products of a single circRNA may be affected by multiple *trans*-factors. When co-expressing these *trans*-factors with the circPFAS containing mutation on its IRES-like element (AAGAAG), we found that the translation enhancing activities of PABPC1, hnRNP A1 and ELAVL1 were dependent on the IRES-like hexamer in

circPFAS, whereas the effect of hnRNP U is independent on this IRES-like element (Fig. 5G and Fig. S6D). This deference is probably because these factors bind to the IRES-like hexamer with distinct specificities and affinities, or due to subtle differences of the mechanism by which various factors affect circRNA translation.

Discussion

Several recent studies indicated that some circRNAs can function as template to direct protein synthesis, however the nature of circRNA translation is still under debate because other studies failed to detect the significant association of circRNA with polysome [3,37,38]. In addition, the mechanism of circRNA translation is not clear. While the cap-independent translation of circRNA generally requires a viral or endogenous IRES, we have demonstrated that a short element containing m6A modification site is sufficient to drive circRNA translation by directly recruiting initiation factors [13]. Here we surprisingly found that the requirement of IRESs can be easily fulfilled, and many short sequences (~2% of all hexamers) are capable of driving cap-independent translation in circRNAs. In fact, any circRNAs longer than 50-nt should contain an IRES-like hexamer by chance, and more importantly endogenous circRNAs are enriched with such IRES-like elements compared to linear mRNAs. As a result, thousands of cytoplasmic circRNAs can be potentially translated, among which hundreds of circRNA-coded peptides were supported by mass spectrometry evidences. We further identified many RNA binding proteins that can specifically recognize these IRES-like short elements and function as *trans*-factor to promote cap-independent translation, providing a new paradigm on the mechanism of circRNA translation.

The majority of the identified translatable circRNAs code for new protein isoforms overlapping with canonical gene products, 50% of which can produce protein concatemers through a rolling circle translation. This finding raises an

interesting open question regarding the biological function of the circRNA-coded protein isoforms. Because these circRNA-coded isoforms have large overlap with the canonical host genes, the circRNA-coded isoforms may function as competitive regulator of canonical isoforms or play the similar function in different subcellular location. On the other hand, the protein concatemers translated from circRNAs may also function as scaffold for assembly of large complexes, or form protein aggregations that are toxic to cells.

Compared to linear mRNAs, a relatively small number of circRNAs are reported to be associated with polysomes [37,38], suggesting an inefficient translation of circRNAs. In addition, the minimal requirement for the cap-independent translation of circRNAs and the difficulties to detect circRNA-coded products presented an intriguing paradox. While there is no clear explanation, several factors may help to reconcile such contradiction. First, although most circRNAs have the capacity to be translated, it does not necessarily mean that they are indeed translated efficiently *in vivo* to produce stable proteins. It is possible that some products from pervasive translation of circRNAs may not be folded correctly and thus be rapidly degraded. This scenario is conceptually similar to the pervasive transcription occurred in many genomic regions on both directions, where most of the transcribed products are degraded and only a small fraction of products are stable and functional [39,40]. In support of this notion, we found that the short C-terminal tails specifically encoded by circRNA sequences across the back splice sites can indeed cause rapid protein

degradations (Fig. S5D). In another word, the protein folding and stability may function as the quality control step for circRNA translation.

The other possibility is that the initiation of cap-independent translation of circRNAs is less efficient than linear mRNAs, but the translation elongation rate should be comparable between circular *vs.* linear RNAs once the active ribosomes are assembled onto mRNAs. As a result, the translation of most circRNAs may be carried out by monoribosomes rather than by polysomes, which could explain the lack of circRNAs in polysome-associated RNAs. This is supported by the observation that rolling circle translation of the reporter circRNA has produced much more products than the same circRNA containing stop codon (Fig. 2B and 2C), the latter of which requires reinitiation at each round of translation. Consistent with this notion, we have observed a larger fraction of circRNA-coded peptides from rolling circle translation in the analyses of mass spectrometry dataset (Fig. 4D vs Fig. 4B), suggesting that products of rolling circle translation are relatively more abundant.

We have, for the first time, identified and validated the rolling circle translation products of several circRNAs (Fig. 5). Because such proteins contain concatemeric repeats, they are probably misfolded to form protein aggregates that may have pathogenic properties. On the other hand, the misfolded protein products often induce unfolded protein response that leads to protein degradation and apoptosis (Yang et al, unpublished data). We think the biological functions of the circRNAs with rolling circle ORFs will be an important subject for future study, however it is beyond the scope of this study.

It is well accepted that the translation through cap-independent pathways are less efficient under normal physiological condition. However under certain cellular stress condition (like heat stress) or in certain cell types (like cancer cells), the canonical cap-dependent translation is inhibited and the cap-independent translation may become more predominant [41,42]. Consistently we found that the translation of GFP from circRNA is promoted in heat shock conditions [13], suggesting that circRNA-coded proteins may be induced under such conditions (or in certain cells where canonical translation is suppressed), implying potential roles for the circRNA-coded proteins in stress response and cancer cell progression.

Methods Summary (see supplementary material for detailed methods)

Plasmid library construction and screening

In order to screen short elements for the initiation of circRNA translation, the previously described pcircGFP reporter [12] was modified and inserted with a random 10mer sequence library. We obtained sufficient numbers of *E. coli* clones to achieve ~2-fold coverage of all possible decamers. The resulting library was transfected into 293T cells (20 μg/ per 15 cm dish) and the green cells were sorted at 48 hours after transfection. In total 122 million cells were sorted, we collected 4 million cells without GFP fluorescence (negative controls), 13 million cells with low GFP fluorescence, 5 million cells with medium GFP fluorescence and 0.5 million cells with high GFP. Then RNAs were extracted, and sequencing library was generated by RT-PCR. RNA-seq was performed with Hiseq 2500.

Identification of enriched motifs in IRES-like elements

We used a statistic enrichment analysis to extract enriched motifs from decamer sequences recovered in green cells. Briefly, each inserted 10-mer was extended into a 14-mer by appending 2-nt of the vector sequence at each end to allow for cases in which IRES activity derived from sequences overlapping the vector. The resulting 14-nt sequences were broken into overlapping hexamers, and the enrichment score of each 6-mer between different datasets was calculated using Z-test. Hexamers with score > 7 are defined as IRES-like elements, while the hexamers with score < -7 are defined as depleted elements.

Identification of *trans*-factors with RNA affinity purification

The RNA affinity purification method was adopted from the previously described protocol [21]. Each biotin labeled RNA sample was incubated with cell extracts of 2.5 × 10^8 HeLa cells for 2 hrs at 4 °C in a 5 ml mixture. Next, 50 µl Streptavidin-agarose beads were added into the mixture and incubated for 2 hrs at 4 °C with slow rotation. The beads were washed 3 times and eluded, and the total proteins were then separated with a 4-20% PAGE Gel for mass spectrometry analysis.

circORF prediction

All potential ORFs encoded by the circRNAs in three reading frames of the sense strand were predicted. We set a threshold of ORF length at ⩾20aa. If one ORF doesn't contain stop codon, it was defined as rolling circle ORF (rcORF, i.e. an infinite ORF can be translated through rolling circle fashion).

We used the blastp 2.6.0+ to detect the homologues of circRNA-coded ORFs in non-redundant protein database. If no homologous proteins were detected for the circORFs, we labeled the circRNA as "blast null". If circORF is partially overlapped with host ORF (at least 7aa are the same), we named it "overlapped circORF", if the circORF do not overlap with the host protein but are homologous to other known proteins, we named it "homologous circORF".

Identification of circRNA-coded proteins

Using an open search engine, pFind(v3.1.3) [34], we searched two previous published human comprehensive proteome datasets [32,33] against a combined database containing all UniProt human proteins and the potential circRNA-coded peptides across back splice junctions from all three frames. The circRNAs were collected from circBase combining with the dataset of full length circRNAs [20,26]. We selected positive mass spectra across back splice junction using following thresholds: q $\leqslant$ 0.01, peptides length $\geqslant$ 8, missed cleavage sites $\leqslant$ 3, allowing only common modifications (cysteine carbamidomethylation, oxidation of methionine, protein N-terminal acetylation, pyro-glutamate formation from glutamine, and phosphorylation of serine, threonine, and tyrosine residues). We considered potential ORFs with 'NTG' as start codon because non-ATG start is common in IRES-mediated translation. The resulting peptides were searched against non-redundant human protein database using blastp-short and the peptides with less than two mismatches from known proteins were removed. Finally, we used a strict cutoff to select positive spectra in which the circRNA-coded peptides were broken into fragment ions at both sides of back splice junction.

For control peptides encoded by corresponding linear mRNAs, we selected the 5′ and 3′ splice junctions adjacent to the back-splicing junctions of all circRNAs, and used identical pipeline and cutoff to search the same MS-MS datasets for peptides encoded by the adjacent splice junctions. The resulting mass spectra supporting peptides across the canonical splice junctions adjacent to the circRNAs were further analyzed.

Data availability

Four published circRNA datasets (Fig. 2A, and 4A) were retrieved from circBase (http://circbase.org/). The full-length circRNA dataset (Fig. 4B and D) was obtained from the published ribominus RNA-seq data that was generated from the RNase R treated RNAs of HeLa cells (BioProject database of Genbank, accession number PRJNA266072).

Two human comprehensive proteome datasets (Fig. 4D-G, and Fig. S5A-B) were obtained from Bekker-Jensen, DB, et al, and Kim, MS, et al. & Pinto, SM, et al., which in turn rely on freely available data obtained from PRIDE Archive(accession number : PXD004452, and PXD000561)

All data supporting the findings of this study are available from the corresponding authors on reasonable request.

Code availability

The code used for analyzing data is available from the corresponding authors on reasonable request.

Acknowledgment

The authors want to thank Dr. Hao Chi for his support in identifying circRNA-coded peptides from proteomic data using open pFind(v3.1.3) software, Dr. Fangqing Zhao for sharing the unpublished full length circRNA dataset, Ms. Yue Hu for help in analyzing RBP binding data, and Drs. Reinhard Lührmann and Xiaoling Li for useful discussions and comments. This work is supported by National Natural Science Foundation of China to Z.W. (31570823, 31661143031, and 31730110) and Y.Y. (91753135, 31870814). Z.W. is also supported by the type A CAS Pioneer 100-Talent program. Y.Y. is also sponsored by the Youth Innovation Promotion

Association CAS and Shanghai Science and Technology Committee Rising-Star Program (19QA1410500).

Author Contributions

Conceptualization, Z.W. and Y.Y; Methodology, X.F., Y.Y., and Z.W.; Software, X.F.; Experiments, X.F., Y.Y.; Writing, X.F., Y.Y., X.L. and Z.W.; Funding Acquisition, Y.Y., and Z.W.

Declaration of Interests

Z. W. and Y. Y. has co-founded a company, CirCode Biotech, to commercialize the application of circular RNA as template of protein production/expression. The other authors declare no competing financial interests.

Reference

1. Chen, L.L. The biogenesis and emerging roles of circular RNAs. *Nat Rev Mol Cell Biol* **17**, 205-11 (2016).
2. Barrett, S.P. & Salzman, J. Circular RNAs: analysis, expression and potential functions. *Development* **143**, 1838-47 (2016).
3. Jeck, W.R. et al. Circular RNAs are abundant, conserved, and associated with ALU repeats. *RNA* **19**, 141-57 (2013).
4. Salzman, J., Gawad, C., Wang, P.L., Lacayo, N. & Brown, P.O. Circular RNAs are the predominant transcript isoform from hundreds of human genes in diverse cell types. *PLoS One* **7**, e30733 (2012).
5. Li, X., Yang, L. & Chen, L.L. The Biogenesis, Functions, and Challenges of Circular RNAs. *Mol Cell* **71**, 428-442 (2018).
6. Hansen, T.B. et al. Natural RNA circles function as efficient microRNA sponges. *Nature* **495**, 384-8 (2013).
7. Memczak, S. et al. Circular RNAs are a large class of animal RNAs with regulatory potency. *Nature* **495**, 333-8 (2013).
8. Ashwal-Fluss, R. et al. circRNA biogenesis competes with pre-mRNA splicing. *Mol Cell* **56**, 55-66 (2014).
9. Li, Z. et al. Exon-intron circular RNAs regulate transcription in the nucleus. *Nat Struct Mol Biol* **22**, 256-64 (2015).
10. Zhang, Y. et al. Circular intronic long noncoding RNAs. *Mol Cell* **51**, 792-806 (2013).
11. Chen, C.Y. & Sarnow, P. Initiation of protein synthesis by the eukaryotic translational apparatus on circular RNAs. *Science* **268**, 415-7 (1995).
12. Wang, Y. & Wang, Z. Efficient backsplicing produces translatable circular mRNAs. *RNA* **21**, 172-9 (2015).
13. Yang, Y. et al. Extensive translation of circular RNAs driven by N(6)-methyladenosine. *Cell Res* **27**, 626-641 (2017).
14. Legnini, I. et al. Circ-ZNF609 Is a Circular RNA that Can Be Translated and Functions in Myogenesis. *Mol Cell* **66**, 22-37 e9 (2017).
15. Pamudurti, N.R. et al. Translation of CircRNAs. *Mol Cell* **66**, 9-21 e7 (2017).
16. Gilbert, W.V. Alternative ways to think about cellular internal ribosome entry. *J Biol Chem* **285**, 29033-8 (2010).
17. Kozak, M. A second look at cellular mRNA sequences said to function as internal ribosome entry sites. *Nucleic Acids Res* **33**, 6593-602 (2005).
18. Kozak, M. Lessons (not) learned from mistakes about translation. *Gene* **403**, 194-203 (2007).
19. Weingarten-Gabbay, S. et al. Systematic discovery of cap-independent translation sequences in human and viral genomes. *Science* **351**(2016).
20. Glazar, P., Papavasileiou, P. & Rajewsky, N. circBase: a database for circular RNAs. *RNA* **20**, 1666-70 (2014).
21. Wang, Y. & Wang, Z. Systematical identification of splicing regulatory cis-elements and cognate trans-factors. *Methods* (2013).
22. Wang, Y., Ma, M., Xiao, X. & Wang, Z. Intronic splicing enhancers, cognate splicing factors and context-dependent regulation rules. *Nat Struct Mol Biol* **19**, 1044-52 (2012).

23. Wang, Y. et al. A complex network of factors with overlapping affinities represses splicing through intronic elements. *Nat Struct Mol Biol* **20**, 36-45 (2013).
24. Yang, Y. & Wang, Z. Constructing GFP-Based Reporter to Study Back Splicing and Translation of Circular RNA. *Methods Mol Biol* **1724**, 107-118 (2018).
25. Rybak-Wolf, A. et al. Circular RNAs in the Mammalian Brain Are Highly Abundant, Conserved, and Dynamically Expressed. *Mol Cell* **58**, 870-85 (2015).
26. Gao, Y. et al. Comprehensive identification of internal structure and alternative splicing events in circular RNAs. *Nat Commun* **7**, 12060 (2016).
27. Schuller, A.P. & Green, R. The ABC(E1)s of Ribosome Recycling and Reinitiation. *Mol Cell* **66**, 578-580 (2017).
28. Heuer, A. et al. Structure of the 40S-ABCE1 post-splitting complex in ribosome recycling and translation initiation. *Nat Struct Mol Biol* **24**, 453-460 (2017).
29. Harvey, R.F. et al. Trans-acting translational regulatory RNA binding proteins. *Wiley Interdiscip Rev RNA* **9**, e1465 (2018).
30. Wei, H. & Wang, Z. Engineering RNA-binding proteins with diverse activities. *Wiley Interdiscip Rev RNA* **6**, 597-613 (2015).
31. Wigington, C.P., Williams, K.R., Meers, M.P., Bassell, G.J. & Corbett, A.H. Poly(A) RNA-binding proteins and polyadenosine RNA: new members and novel functions. *Wiley Interdiscip Rev RNA* **5**, 601-22 (2014).
32. Bekker-Jensen, D.B. et al. An Optimized Shotgun Strategy for the Rapid Generation of Comprehensive Human Proteomes. *Cell Syst* **4**, 587-599 e4 (2017).
33. Kim, M.S. et al. A draft map of the human proteome. *Nature* **509**, 575-81 (2014).
34. Chi, H. et al. Comprehensive identification of peptides in tandem mass spectra using an efficient open search engine. *Nat Biotechnol* (2018).
35. Maass, P.G. et al. A map of human circular RNAs in clinically relevant tissues. *J Mol Med (Berl)* **95**, 1179-1189 (2017).
36. Preusser, C. et al. Selective release of circRNAs in platelet-derived extracellular vesicles. *J Extracell Vesicles* **7**, 1424473 (2018).
37. Guo, J.U., Agarwal, V., Guo, H. & Bartel, D.P. Expanded identification and characterization of mammalian circular RNAs. *Genome biology* **15**, 409 (2014).
38. You, X. et al. Neural circular RNAs are derived from synaptic genes and regulated by development and plasticity. *Nature neuroscience* **18**, 603-10 (2015).
39. Jensen, T.H., Jacquier, A. & Libri, D. Dealing with pervasive transcription. *Mol Cell* **52**, 473-84 (2013).
40. Wade, J.T. & Grainger, D.C. Pervasive transcription: illuminating the dark matter of bacterial transcriptomes. *Nat Rev Microbiol* **12**, 647-53 (2014).
41. Leprivier, G., Rotblat, B., Khan, D., Jan, E. & Sorensen, P.H. Stress-mediated translational control in cancer cells. *Biochimica et biophysica acta* **1849**, 845-60 (2015).
42. Liu, B. & Qian, S.B. Translational reprogramming in cellular stress response. *Wiley Interdiscip Rev RNA* **5**, 301-15 (2014).

Figures and Figure Legends

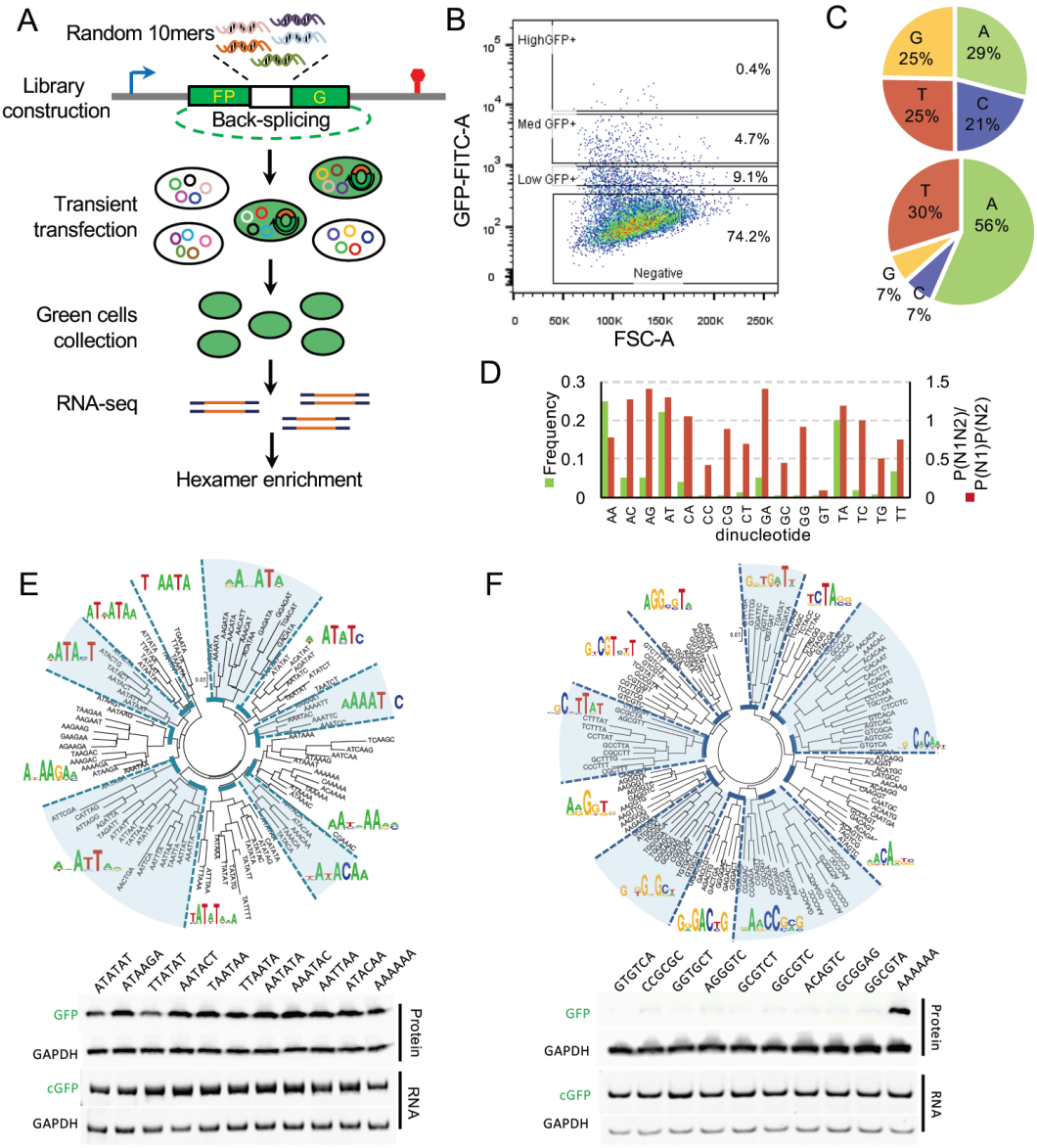

Figure 1. Extensive IRES-like elements can drive circRNA translation.

(A) Schematic diagram for screening short IRES-like elements. Random decamers were inserted into pcircGFP-BsmBI reporter, and the resulting library was transfected into 293T cells and sorted by FACS. The green cells were collected and the inserted sequences were sequenced using high-throughput sequencing. The hexamers enriched in green cells were identified by computational analysis (also see method).

(B) Flow-cytometry analysis of cells transfected with circRNA reporter containing the random 10-mer library. The cells were classified into four groups based on their GFP fluorescence (GFP negative cells and cells with low, medium or high GFP signals). The cells with medium and high fluorescence were sorted as "green cells".

(C) Single nucleotide frequency in the starting library (top) and the sequences enriched in green cells (bottom).

(D) Dinucleotide frequency and enrichment of the sequences enriched in green cells.

(E) The 97 enriched hexamers (i.e., IRES-like elements, z score >7) were clustered into 11 groups with the consensus motifs shown as pictogram (top). The representative hexamers in each cluster were inserted back into the circRNA reporter, and the resulting reporters that were transiently transfected into 293T cells. The translation of GFP was assayed by western blot at 48 hours after transfection (bottom).

(F) The 122 depleted hexamers (i.e., negative control, z score < -7) were clustered into 11 groups and the consensus motifs were shown as pictogram (top). The activities of representative hexamers in all clusters were tested using the same condition as panel E. An IRES-like element, AAAAAA, was included as the positive control.

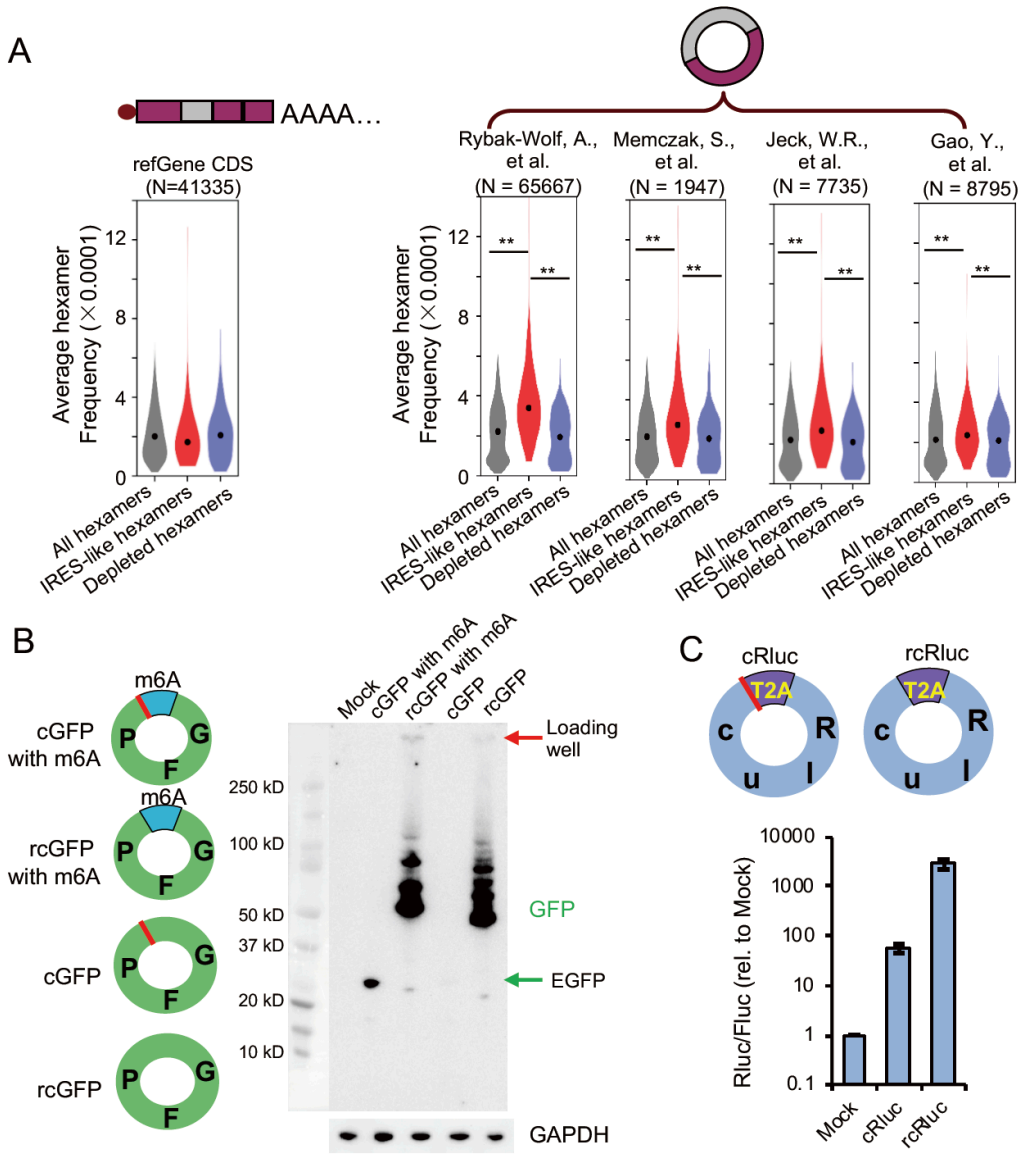

Figure 2. circRNAs contain many IRES-like elements that initiate translation.

(A) IRES-like elements are significantly enriched in circRNAs. Average frequencies of different types of hexamers (all hexamers, IRES-like hexamers and depleted hexamers) in linear mRNAs *vs.* circRNAs were plotted. N: the number of RNA sequences in each dataset. **: p-value < 0.001 with Kolmogorov–Smirnov test.

(B) Translation of circRNAs can be initiated by internal coding sequence. Left panel, schematic diagrams of four reporter circRNAs that code for GFP. From top to bottom: circRNA with an m6A site at upstream of the start codon; circRNA with an upstream m6A site and no stop codon; circRNA with start codon immediately following the stop codon; circRNA containing only the coding sequence (no stop codon or UTR).

Red line indicates stop codon. Right panel, western blot analysis to detect translation products from circRNAs. The circRNA plasmids were transfected into 293T cells, and samples were analyzed by western blot at 2 days after transfection. Both rcGFP with m6A and rcGFP can generate several large protein concatemers of GFP through rolling circle translation. The level of GAPDH was measured as a loading control.

(C) Translation of the circRNA-coded Renilla luciferase (Rluc) using internal IRES-like elements. Top: schematic diagram of two Rluc circRNAs. cRLuc contains a sequence coding a T2A peptide by which the translation product can be cleaved into full length Rluc protein. rcRluc does not contain stop codon. Bottom: dual luciferase assay of cRluc and rcRluc. Control and circular Rluc plasmids were co-transfected with Fluc (firefly luciferase) reference reporter into 293T cells. The cells were lysed at 48 hours after transfection for luminescence measurement using luminescence reader, and the relative luminescence signals were plotted (mean ± SD, n = 3 independent experiments).

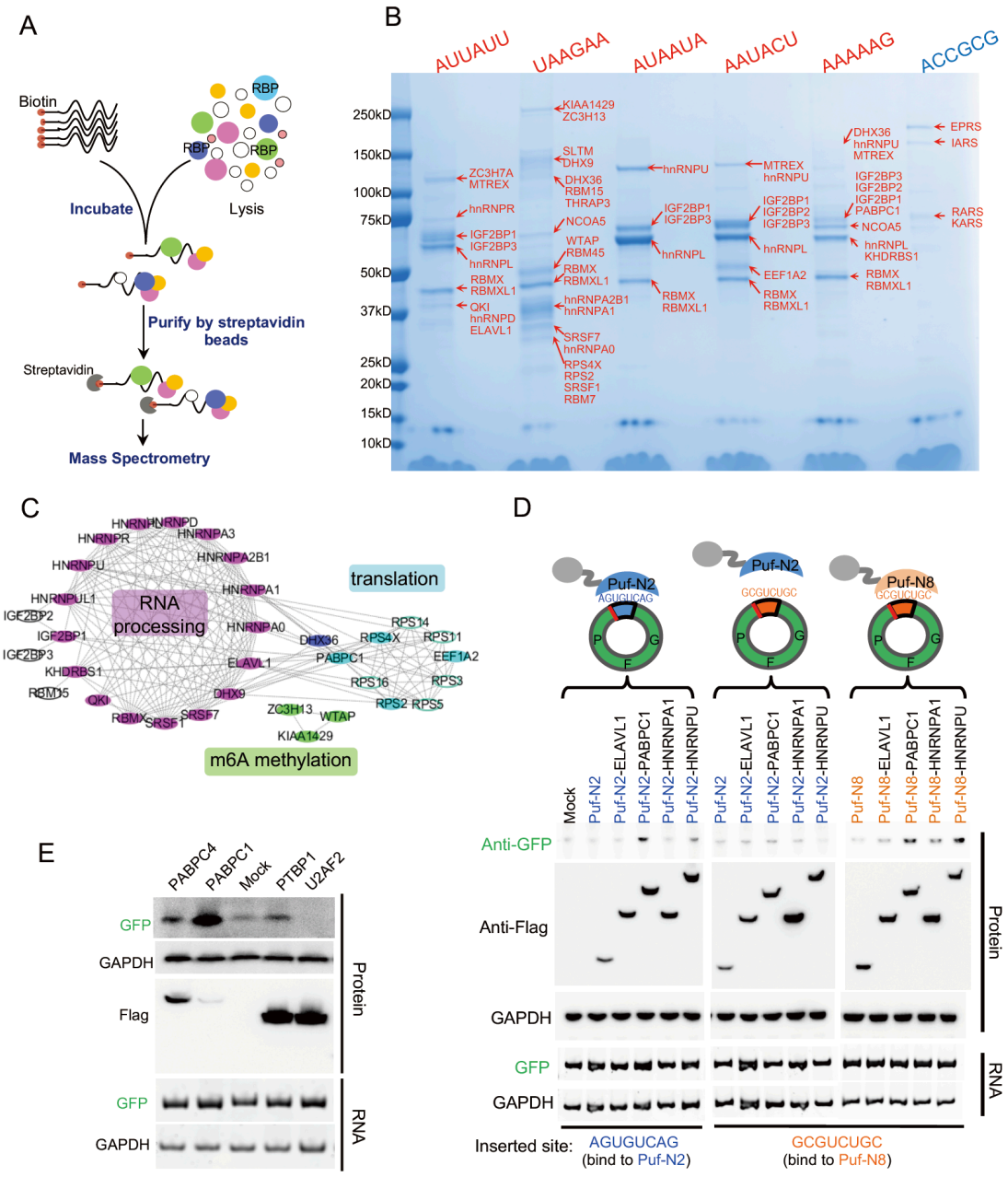

Figure 3. Systematically identification of *trans*-factors that recognize IRES-like elements.

(A) Schematic diagram of RNA affinity purification. Biotin-labeled RNAs containing consensus motifs of IRES-like elements were incubated with HeLa cell lysate, and RNA-protein complexes were purified by streptavidin beads. The proteins were further identified by mass spectrometry (see method for details).

(B) Identification of *trans*-factors bound by each RNA probe. The probes presenting five consensus motifs of IRES-like elements (red) and a control probe (blue) were

used (see table S2 for full sequence). The total proteins eluded from each RNA probe were separated with SDS-PAGE, and each band was cut and analyzed by mass spectrometry. The top three identified proteins in each band were labeled at right in red.

(C) Protein-protein interaction network of identified *trans*-factors. Top proteins bound by all RNA probes (i.e., IRES-like elements) were analyzed by STRING and clustered into two main groups by MCODE tool.

(D) Measurement of the activity of *trans*-factors. The circRNA reporter inserted with two depleted hexamers in tandem (with very weak IRES-activity by itself) were co-transfected into 293T cells with different Puf-fusion proteins that specifically recognize an 8-nt target in the inserted sequences. The resulting cells were collected at 2 days after transfection to analyze the protein and RNA levels by western blot and RT-PCR respectively. Different pairs of Puf proteins and 8-nt targets were used as specificity control. Puf-N2 can specifically bind AGUGUCAG, whereas Puf-N8 can specifically bind to GCGUCUGC.

(E) Validation of PABPC1 activity. The expression vector of PABPC1 and various control RBPs were co-transfected with circRNA translation reporter containing $(A)_{10}$ sequence before the start codon, and the protein products were assayed at 48 hours after transfection.

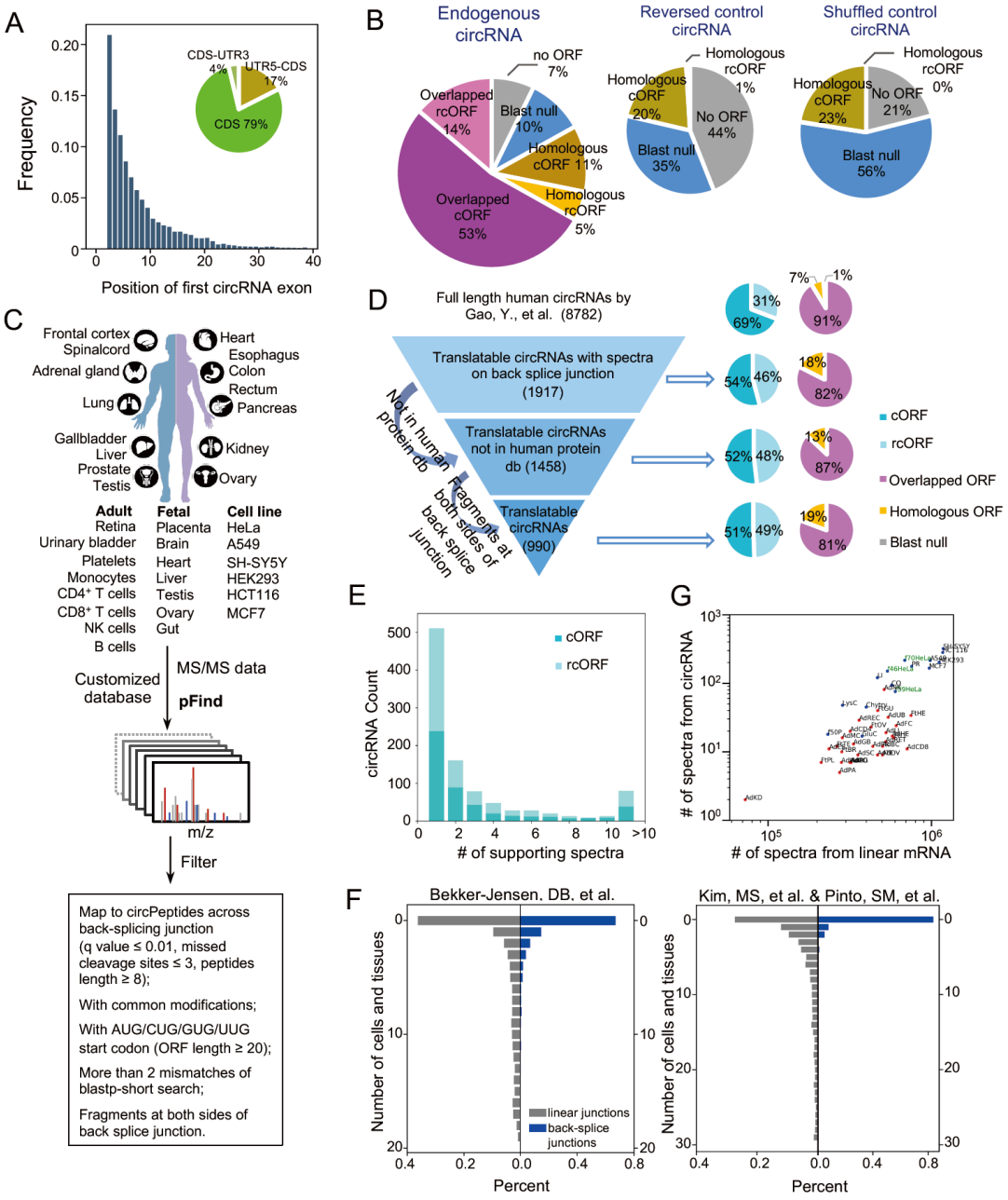

Figure 4. Identification of circRNA-coded proteins.

(A) Position distribution for the first exon of circRNAs in their host genes. Full length circRNA sequences were analyzed based on previously published datasets, and the histogram was plotted according to the position of the first circRNA exon (i.e., the exon number) in host genes. The inserted pie chart presents the percent of circRNAs overlapping with different regions of mRNA.

(B) Survey of the potential coding products of circRNAs. Left panel, percent of endogenous circRNAs that code for an ORF longer than 20 aa. Purple pie slices:

circRNAs translated in a regular fashion (cORF, dark purple) or a rolling circle fashion (rcORF, light purple) into proteins that are partially overlapped with their host genes; brown pie slices: circRNAs translated in a regular fashion (cORF, dark brown) or a rolling circle fashion (rcORF, light brown) into proteins that are not overlapped with their host genes but are homologous to other known proteins; blue pie slices: circRNAs translated into proteins that are not homologous to any known proteins (cORF and rcORF combined); grey pie slices: circRNAs do not contain any potential ORF longer than 20 aa. Right panels: the same analysis of putative coding products from two control circRNA sets, reversed sequences of endogenous circRNAs and random shuffled sequences of endogenous circRNAs.

(C) Schematic diagram for identification of circRNA-coded proteins using proteomic datasets.

(D) Schematic diagram of translatable circRNA identification pipeline. Left, computational filters sequentially applied to identify translatable circRNAs, the numbers of circRNAs passing each filter. Right, the percentage of different types of circRNA-coded ORFs (rcORFs, cORFs, overlapped ORFs, homologous ORFs, and blast null) in total circRNAs that passed each filter. The definition of different types of ORFs encoded by circRNAs are same as panel B.

(E) Distribution of the supporting spectra for each translatable circRNA.

(F) Distribution of the number of cell lines and tissues for each translatable circRNA in two proteomic datasets.

(G) Comparison of the numbers of spectra from linear mRNAs vs. circRNAs. Abbreviation of different tissues and cell lines are listed in table S4. Blue dot: proteomic data from Bekker-Jensen, DB, et al; Red dot: proteomic data from Kim, MS, et al. & Pinto, SM, et al.. Green words indicate the 39 fractions, 46 fractions and 70 fractions from HeLa cells using high-capacity offline HpH reversed-phase LC.

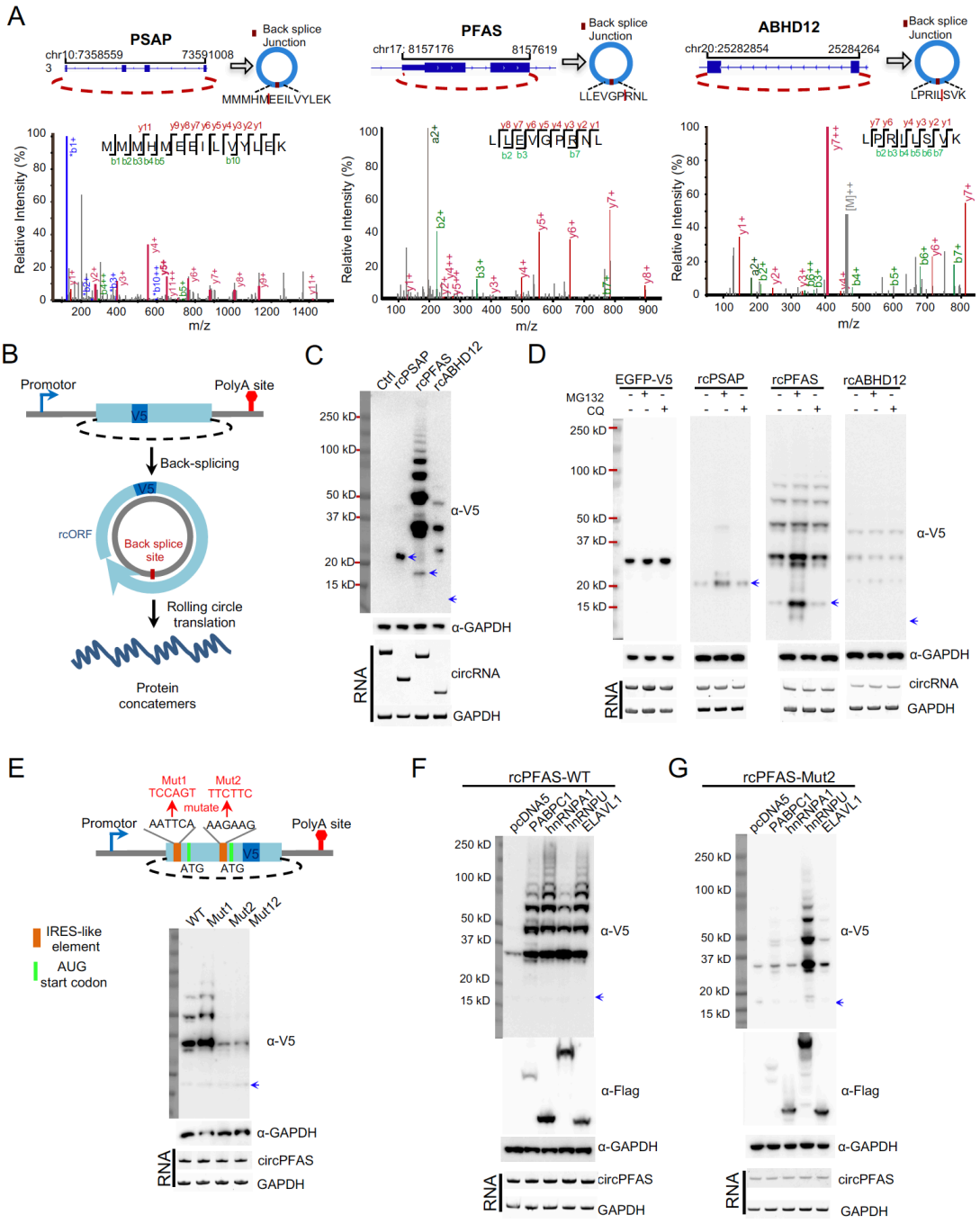

Figure 5. Rolling circle translation of endogenous circRNAs.

(A) The higher-energy collisional dissociation (HCD) MS/MS spectrum of the peptide across the back splice junction of the human circPSAP (MMMHMEEILVYLEK), circPFAS (LLEVGPRNL), and circABHD12 (LPRILSVK). The annotated b- and y-ions are marked in red and green color, respectively.

(B) Schematic diagram of rcORF translation reporters. The coding region of the endogenous rcORF was inserted into a back-splicing reporter. To detect the translation products from endogenous rcORF, a V5 epitope tag was inserted into the same reading frame of the rcORF. After back-splicing, the circRNA containing a rcORF and an in-frame V5 epitope tag was translated through rolling circle fashion to produce the protein concatemers.

(C) The back-splicing reporters containing three endogenous rcORFs were transfected into 293 cells, the cells were collected at 48 hours after transfection, and the levels of circRNA-coded proteins and circRNAs were detected by western blotting and RT-PCR, respectively. The blue arrows represent the predicted molecular weight of the single cycle of translation product derived from cPSAP (22.4kD), cPFAS (15.6kD), or cABHD12 (10.5kD).

(D) The translation products of rolling circle translation were degraded through proteasome pathway. The rcORF translation reporters were transfected into 293T cells. The transfected cells were treated with 10 μM MG132 for 2 hours, or 10 μM chloroquine for 4 hours before cell collection.

(E) The translation of rcPFAS was reduced by mutations on IRES-like elements of the circPFAS. The circPFAS contains two IRES-like hexamers (AATTCA and AAGAAG), which were mutated into neutral sequences (mut1 and mut2). Different circRNA reporters were transfected into 293T cells and the RNAs and proteins were detected using similar procedure as described in panel C.

(F) Co-expression of *trans*-acting factors increased the rolling circle translation products. The back-splicing reporter of rcPFAS was co-transfected into 293T cells with the expression vectors of various *trans*-acting factors that bind to the newly-identified IRES-like elements. The cells were collected and analyzed using same procedures as described in panel C.

(G) The circRNA with mutated IRES-like hexamer AAGAAG (Mut2) was co-expressed with same set of *trans*-acting factors, and the production of rolling circle translation were measured using same experimental conditions described in panel F.